Bond Alternation and Aromatic Character in Cyclic Polyenes: Assessment of Theoretical Methods for Computing the Structures and Energies of Bismethano[14]annulenes

Maja Nendel,[†,‡] K. N. Houk,*[,†] L. M. Tolbert,*[,‡] Emanuel Vogel,[§] Haijun Jiao,[||] and Paul von Ragué Schleyer*[,||]

Department of Chemistry and Biochemistry, University of California—Los Angeles, Los Angeles, California 90095-1569, School of Chemistry and Biochemistry, Georgia Institute of Technology, Atlanta, Georgia 30332-0400, Institut für Organische Chemie, Universität zu Köln, Greinstrasse 4, D-50939 Köln, Germany, and Computer-Chemie-Centrum, Institut für Organische Chemie, Universität Erlangen-Nürnberg, Henkestrasse 42, D-91054 Erlangen, Germany

Received: May 4, 1998

The *syn* and *anti* bismethano[14]annulenes have been used to test the accuracy of the semiempirical (PM3) and ab initio (HF and MP2), as well as density functional theory (BLYP and B3LYP) methods. Compared to experimental data, PM3 and HF overemphasize bond localized structures, while the correlated MP2 and density functional methods tend to favor overly delocalized aromatic structures. B3LYP computations give the best agreement with the available experimental data, they provide the most reliable estimates of the relative energies of aromatic and non-aromatic cyclenes. The calculated magnetic susceptibility exaltations and nucleus-independent chemical shifts (NICS) parallel geometric and energetic criteria. The methods were also applied to 1,6-methano[10]annulene and azulene.

Introduction

Aromaticity is expressed by a combination of properties in cyclic delocalized systems.[1] The relationships among the number of π electrons, stability, and reactivity have been central subjects in organic chemistry ever since Hückel provided a theoretical basis for the concept of aromaticity which led to the $(4n + 2)$ π electron rule. Recently, Schleyer et al. established linear relationships among different measures of aromaticity (such as stabilization, bond length equalization, and magnetic susceptibility exaltation, as well as nucleus-independent chemical shifts (NICS)) for a wide-ranging set of aromatic and antiaromatic five-membered ring heterocycles.[2,3] In general, aromatic systems with cyclic delocalized electrons are stabilized, independent if these electrons have a π, σ, or hybrid character. The systems have equalized bond lengths and exhibit exalted magnetic susceptibilities relative to the nonaromatic analogs.

The origin of the bond length equalization is still being debated. Shaik et al. and others maintain that the π bonds are in fact distortive, while the symmetric structure of benzene is solely due to the σ skeleton.[4] Weinhold et al. came to the conclusion that both, σ and π bond effects, work together in order to equalize the bond lengths.[5]

There have been many recent theoretical studies on large aromatic systems such as the C_n linear, cyclic, and fullerene structures.[6,7] The daunting sizes of many systems of interest prohibit the use of the most sophisticated ab initio treatments (e.g., coupled cluster methods). Consequently, density functional theory (DFT) has become a popular method to study such molecules. However, there are systematic problems with many theoretical models; some overemphasize bond length equalization and aromaticity, while others underestimate the stabilization. We have recently described the geometrical performance of various methods on bridged [14]-annulenes, concluding that of the economical methods, only B3LYP provides a reasonable balance between delocalized and localized structures.[7c] Kertesz et al. have provided an extensive study of [14]- and [18]-annulenes, with several methods and more recently the whole set of annulenes up to [66]annulene![7e] Recent comparisons of methods for delocalized systems stress the importance of correlation,[8] but not all correlated methods guarantee a balanced treatment.[7c−e,9]

Most theoretical methods reproduce the benzene geometry well, but the aromatic stabilization energies [ASE, based on the homodesmotic equation: 3 (trans-butadiene−ethylene) = benzene)] are generally overestimated compared to the experimental results.[10] For example, both HF/6-31G* and MP2/6-31G* overestimate the benzene ASE by 5.0 and 9.2 kcal/mol as compared with an experimental ASE of 19.7 ± 0.2 kcal/mol.[11] In contrast to the conventional ab initio methods, the hybrid density functional method (B3LYP/6-31G*) not only reproduces the benzene geometry (r_{CC} = 1.397 Å) well, but also the ASE (19.5 kcal/mol at 298 K).[12]

How reliable are these common theoretical methods for computing the geometries and energies of larger, more complicated aromatic systems, such as *syn*-1,6:8,13-bismethano[14]-annulene (**1**)[13] and *anti*-1,6:8,13-bismethano[14] annulene (**2**, Figure 1), synthesized by Vogel's group in Cologne in the 1970s?[14]

NMR and X-ray studies showed that **1** is aromatic, based on only slightly alternating bond lengths (1.37−1.42 Å),[15] the downfield ^{1}H-NMR chemical shifts of the ring protons (7.6−7.9 ppm), and the upfield shift of the protons of the methylene bridges (0.9 and −1.2 ppm). The *anti* isomer (**2**) is nonaromatic as defined by strongly alternating bond lengths (1.34−1.50 Å),[16] by the ^{1}H-NMR chemical shifts of the ring protons (6.2 ppm

[†] Department of Chemistry and Biochemistry.
[‡] School of Chemistry and Biochemistry.
[§] Institut für Organische Chemie.
[||] Computer-Chemie-Centrum.

S1089-5639(98)02097-0 CCC: $15.00
Published on Web 08/14/1998

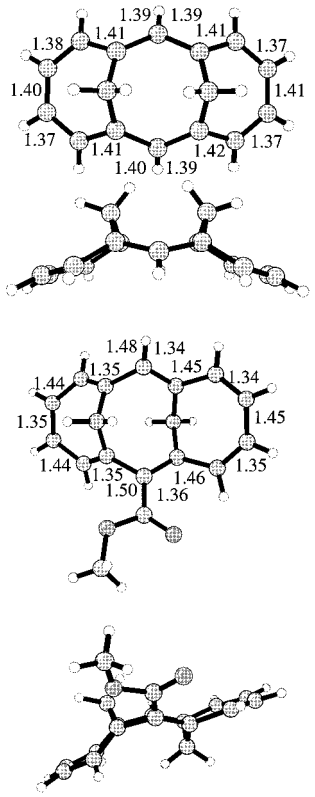

Figure 1. X-ray structures of the *syn*-1,6:8,13-bismethano[14]annulene (**1**) and a derivative (7-methoxycarbonyl) of *anti*-1,6:8,13-bismethano-[14]annulene (**2**). Selected bond lengths are in angstroms.[15,16]

as expected for a localized double bond), and the normal ^{1}H-NMR chemical shifts of the bridging methylene hydrogens (1.9−2.5 ppm). The measured double bond isomerization barrier of the *anti* compound (**2**), probably via an aromatic transition state, is only 7.1 kcal/mol.[14] Hence, such molecules provide excellent tests for different theoretical methods and contribute to the debate about the importance of the σ framework and the π system on equalized bond lengths.

This work quantifies the tendency of various theoretical methods to overestimate or to underestimate stability and delocalization as compared to well-established experimental data. The degree of electron delocalization has been characterized by bond length variations (geometrical criterion) and by magnetic susceptibility exaltations and nucleus independent chemical shifts (magnetic criteria). The ramifications of these results with regard to other recent studies are discussed in the final section of the paper.

Computational Methodology

Semiempirical, ab initio, and density functional computations were performed with Gaussian 94.[17] The MM2* force field calculations used Macromodel.[18] The relative energies are zero point energy (ZPE) corrected in the case of the fully optimized Hartree−Fock (HF) and density functional theory (DFT) structures. The HF ZPEs were scaled by 0.9135.[19] The HF, DFT, and MP2 calculations employed the 6-31G* basis set, unless noted otherwise.

The Julg parameter, A, is used as a measure of the degree of bond length alternation: $A = 1 - (225/n)\Sigma[1-(r_i/r)]^2$, where n is the number of C−C bonds involved in conjugation in the system, r_i the length of individual C−C bonds, and r is the mean C−C bond length.[20] The scaling factor $225/n$ sets A to unity for the structure of benzene with equal C−C bond lengths and to zero for a hypothetical localized form in which the C−C bond lengths alternate between 1.33 and 1.52 Å. The Julg parameter is only one of several means to quantify geometrically the aromaticity of a particular system. Another simple parameter associated directly with bond lengths, Δr_m, is the maximum deviation of the C−C bond length from the mean. Others have used $\sigma = r_{single} - r_{double}$ to assess bond alternation.[7d−h]

In addition to the geometric criteria, the magnetic susceptibility exaltation (Λ) due to cyclic electron delocalization provides highly important evidence for aromaticity.[21] Λ is defined as the difference between the bulk magnetic susceptibility of a compound (χ_M) and the susceptibility a structure without cyclic delocalization ($\chi_{M'}$) estimated from an increment scheme modeling ($\Lambda = \chi_M - \chi_{M'}$). Aromatic compounds have significant (more negative) diamagnetic exaltations; antiaromatic systems, on the other hand, have large (more positive) paramagnetic exaltations; nonaromatics are not exalted.[22]

In this paper, magnetic susceptibilities (χ, in ppm cgs) were calculated uniformly using Kutzelnigg's IGLO (individual gauge for localized orbitals) method with the DZ basis set (constructed from Huzinaga 7s3p set for carbon (4111/21) and 3s set for hydrogen (21)[23] and various optimized geometries. The increment values are taken from ref 24.[24]

The individual ring systems in [14]annulenes were characterized by the nucleus independent chemical shifts (NICS), a simple and efficient aromaticity probe.[3] NICS, the negative of the absolute magnetic shielding, was computed at various ring centers by GIAO-SCF/6-31G* (nonweighted mean of the heavy atom coordinates of the ring) with the Gaussian 94 program. Negative NICS denote aromaticity (−11.5 for benzene) and positive NICS, denote antiaromaticity (28.8 for cyclobutadiene). Nonaromatics have negligible NICS values (−2.1 for cyclohexane). The NICS results agree well with magnetic susceptibility exaltation (Λ) as a criterion of aromaticity. Furthermore, NICS has advantages over Λ. It is less dependent on ring size, and it can be used to assess the aromaticity of individual rings in polycyclic systems. For example, the NICS values for the five- (−21.5) and seven-membered (−8.3) rings of azulene resemble those for the cyclopentadienyl anion (−19.4) and the tropylium ion (−8.2).[3]

Results and Discussion

Because the unsubstituted *anti* compound was not suitable for X-ray structure analysis, the methoxycarbonyl derivative was determined (Figure 1). The *syn* structure (**1**) has C−C bond lengths ranging from 1.37 to 1.42 Å, while the *anti* structure (**2**) has bond lengths between 1.34 and 1.50 Å.[15,16] The corresponding Julg parameters are 0.97 and 0.62, while the maximum deviations of the mean C−C bond lengths are 0.03 and 0.09 Å, respectively. For comparison, the corresponding values are $A = 0.945$ and $\Delta r_m = 0.046$ Å for anthracene,[25] and $A = 0.945$ and $\Delta r_m = 0.029$ Å for naphthalene.[26] Fullerene, the spheroidal weakly aromatic molecule,[27] has bond lengths of 1.38 and 1.45 Å and Δr_m is 0.05 Å.[28] The σ value is 0.07 Å. Aromatics have $\Delta r_m \leq 0.05$ Å, while nonaromatics have $\Delta r_m > 0.05$ Å. Therefore, the *syn* [14]annulene (**1**) is aromatic by all these geometric criteria. The *anti* isomer (**2**) evidently is nonaromatic on the same basis.

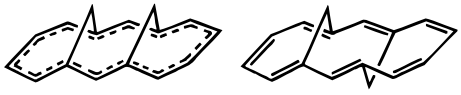

1 **2**

The *syn* (**1**) and *anti* (**2**) structures were fully optimized using a variety of theoretical methods. The notations, **1L**, **1D**, **2L**, and **2D**, refer to the localized and delocalized forms of isomers **1** and **2** (see Figures 2−4). The results for each method are

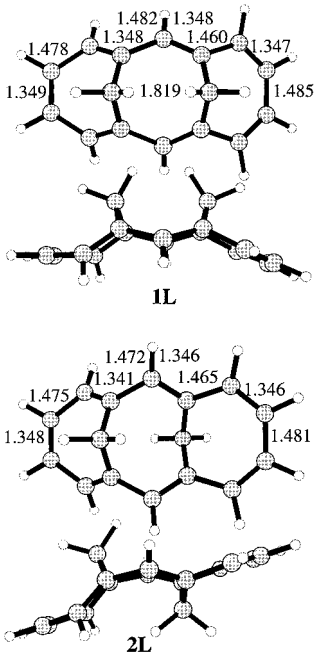

Figure 2. MM2* structures of the localized (**1L**, **2L**) bismethano[14]-annulenes. Selected bond lengths are in angstroms.

described and then compared. The energies and geometries are summarized in Tables 1−2.

MM2*. In a force field with no explicit π calculations like MM2*, only localized structures (**1L** and **2L**) are obtained. The bridged cycloheptatriene unit is nearly flat and the cycloheptadiene subunit is buckled, as in the experimental structure for **2L** (Figure 2). The Julg parameters and the maximum deviation (Δr_m) indicate that both geometries ($A = 0.52$ and $\Delta r_m = 0.07$ Å for **1L** and $A = 0.53$ and $\Delta r_m = 0.07$ Å for **2L**) are similar to the localized X-ray structure ($A = 0.62$ and $\Delta r_m = 0.09$ Å for **2L**). Nonetheless, MM2* provides an estimate of the energy difference between **1L** and **2L**. Unlike **2L**, **1L** has unfavorable steric interactions between the two inner hydrogens of the bismethano bridges. They are estimated to be 8.1 kcal/mol by these calculations.

PM3. PM3 obtains more delocalized structures than MM2* (Figure 3). The PM3 Julg parameters are $A = 0.72$ for **1L** and $A = 0.64$ for **2L**, compared to an $A = 0.62$ for the localized X-ray structure. **2L** is also 5.3 kcal/mol more stable than **1L**. The delocalized **1D** and **2D** are the transition structures for double bond isomerization; they are 9.7 and 33.0 kcal/mol above **1L** and **2L**, respectively. The latter difference reflects the substantial strain in the delocalized *anti* skeleton. Because localized structures are favored by PM3, the difference between **2L** and **2D** is overestimated by 25.9 kcal/mol, based on the experimental value (7.1 kcal/mol) deduced by dynamic ^{1}H-NMR.[14] When this 25.9 kcal/mol error is applied to **1D**, the relative order is consistent with the experimental observation, and **1D** is 10.9 kcal/mol lower in energy than **2L** (Table 1).

Hartree−Fock (HF/6-31G*). The HF/6-31G* results mimic the PM3 data qualitatively. The localized structures (**1L** and **2L**) are favored in both cases, and the delocalized **1D** and **2D** are found to be transition states (Figure 4). As indicated by the Julg parameters ($A = 0.41$ for **1L** and 0.40 for **2L**) and the maximum deviations ($\Delta r_m = 0.07$ Å for **1L** and 0.08 Å for **2L**), the localization is greater than that of the X-ray structure of **2**. The delocalized structures **1D** ($A = 0.93$, $\Delta r_m = 0.03$ Å) and **2D** ($A =$ O.99, $\Delta r_m = 0.02$ Å) have similar parameters to the X-ray *syn* structure (**1**, $A = 0.97$; $\Delta r_m = 0.03$ Å).

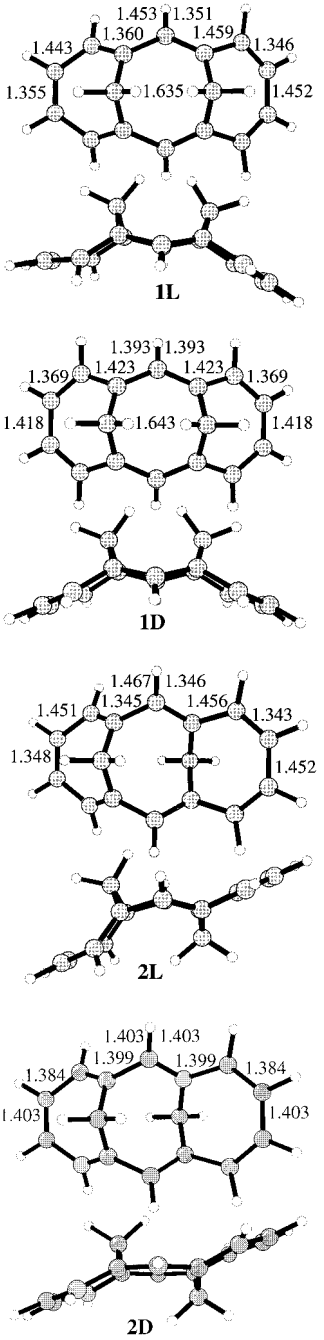

Figure 3. PM3 structures of the localized (**1L** and **2L**) and the delocalized (**1D** and **2D**) bismethano[14]annulenes. Selected bond lengths are in angstroms.

At the HF/6-31G* level, **2L** is only 0.8 kcal/mol lower in energy than **1L**. The barrier for double bond isomerization is 4.6 kcal/mol for **1** and 26.5 kcal/mol for **2**. The error, largely due to the neglect of correlation energy, is thus 19.4 kcal/mol, deduced from the experimental barrier (7.1 kcal/mol) for **2**. This error, 2.8 kcal/mol per electron pair, is smaller than the corresponding values in delocalized pericyclic transition structures (3−4 kcal/mol per electron pair, i.e., the difference between the RHF/6-31G* and the measured barrier).[29] When the calculated energies are corrected, **1D** becomes 14.0 kcal/mol more stable than **2L**. The relative stability order is thus the same as the corrected PM3 order (Table 1).

Both of the HF/6-31G* **1L** and **1D** structures have large Λ values (−35.9 and −84.5), associated with aromaticity (Table 3). **2L** is nonaromatic with a negligible exaltation (−0.2), while

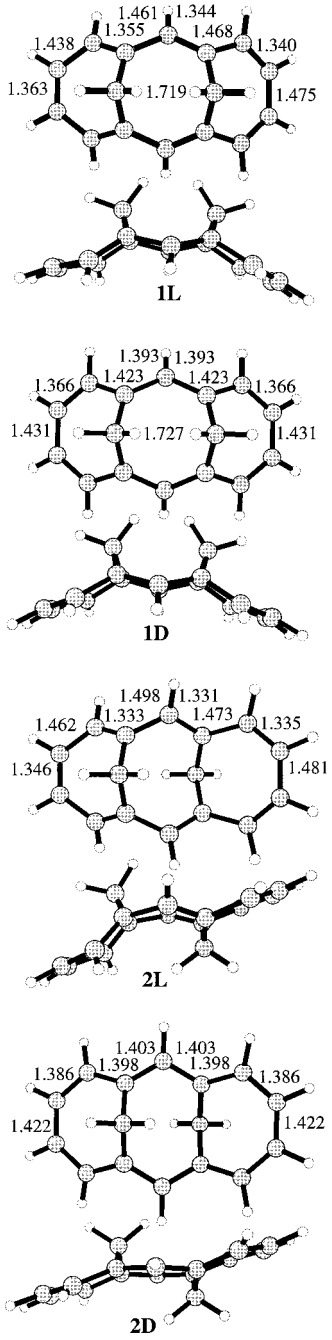

Figure 4. RHF/6-31G* structures of the localized (**1L** and **2L**) and the delocalized (**1D** and **2D**) bismethano[14]annulenes. Selected bond lengths are in angstroms.

the delocalized *anti* structure (**2D**) is the most aromatic (−100.8) of the four structures. In agreement with Λ, the NICS values of **1L** (−13.7 for the central ring, and −8.9 and −4.7 for the outer rings) are similar to those of **1D** (−22.2, −17.0, and −17.0), although they are smaller. Structure **2L** with NICS = −1.5 for the central ring and 0.3 and −5.3 for the two outer rings is definitively nonaromatic. On the other hand, **2D** is highly aromatic with NICS = −17.7 for the central ring and −17.4 for the two outer rings (Table 4).

MP2. The MP2/6-31G*//HF/6-31G* calculations[30] predict that the delocalized structures, **1D** and **2D**, are 13.9 and 6.3 kcal/mol lower in energy than their localized counterparts. Since **2D** is actually 7.1 kcal/mol above **2L**, the MP2 single point calculation overestimates the stability of **2D** by 13.4 kcal/mol.

TABLE 1: Relative Energies (kcal/mol) of Bismethano[14]annulene at Various Levels of Theory

	syn		*anti*		
	1L	**1D**[b]	**2L**	**2D**	E_{err}[c]
exptl[a]			0.0	7.1	0.0
MM2*	8.1		0.0		
PM3	5.3	15.0 (−10.9)	0.0	33.0	−25.9
RHF/6-31G*	0.8	5.4 (−14.0)	0.0	26.5	−19.4
MP2/6-31G*[d]	−8.9	−22.8 (−9.4)	0.0	−6.3	13.4
BLYP/6-31G*	−12.3[e]	−19.8 (−8.5)	0.0[e]	−4.2	11.3
B3LYP/6-31G*	−5.4[f]	−14.6 (−10.5)	0.0	3.0	4.1
B3LYP/6-311+G**[g]	−9.0[h]	−15.2 (−11.8)	0.0	3.7	3.4

[a] Reference 14. [b] Relative energies given in parenthesis are corrected for the error E_{err} (i.e., the difference between **2L** and **1D** with error correction, i.e., Δ(**2L** − **1D**) + E_{err}). [c] The magnitude of the error correction E_{err} is defined as the deviation of the calculated barrier of double bond isomerization from the experimental 7.1 kcal/mol (i.e., E_{err} = 7.1 − Δ(**2D** − **2L**)). [d] MP2/6-31G*//RHF/6-31G*. [e] BLYP/6-31G*//RHF/6-31G* relative to BLYP/6-31G*//RHF/6-31G*. [f] B3LYP/6-31G*//RHF/6-31G* relative to B3LYP/6-31G*//RHF/6-31G*. [g] B3LYP/6-311+G**//B3LYP/6-31G*. [h] B3LYP/6-311+G**//RHF/6-31G* relative to B3LYP/6-311+G**//RHF/6-31G*.

TABLE 2: Geometric Parameters of Bismethano[14]annulene at Various Levels of Theory: *A* (Julg Parameter, Unitless), *r* (Mean C−C Bond Length, angstroms) and Δr_m (Maximum Deviation of Bond Length, angstroms)[a]

	syn			*anti*		
	1L (**1D**)			**2L** (**2D**)		
	A	*r*	Δr_m	*A*	*r*	Δr_m
exptl[b]	(0.97)	(1.39)	(0.03)	0.62	1.40	0.09
MM2*	0.52	1.41	0.07	0.53	1.40	0.07
PM3	0.72	1.40	0.06	0.64	1.40	0.07
	(0.94)	(1.40)	(0.03)	(0.99)	(1.40)	(0.01)
RHF	0.41	1.40	0.07	0.40	1.41	0.08
	(0.93)	(1.40)	(0.03)	(0.99)	(1.40)	(0.02)
BLYP	(0.99)	(1.42)	(0.02)	(0.99)	(1.42)	(0.01)
B3LYP				0.70	1.41	0.07
	(0.98)	(1.41)	(0.02)	(0.99)	(1.41)	(0.01)

[a] The values for the delocalized structures (**1D** and **2D**) are given in parentheses. [b] X-ray structures of *syn* and *anti* bismethano[14]-annulenes.[15,16]

TABLE 3: IGLO/DZ Calculated Magnetic Susceptibilities, χ (Total), and the Magnetic Susceptibility Exaltations, Λ (Total, in ppm cgs) for Various Geometries of Bismethano[14]annulenes[a]

	RHF/6-31G*		BLYP/6-31G*		B3LYP/6-31G*	
	χ (total)	Λ(total)	χ (total)	Λ (total)	χ (total)	Λ (total)
1L	−193.1	−35.9				
1D	−241.7	−84.5	−253.7	−96.5	−250.2	−93.0
2L	−157.4	−0.2			−163.6	−6.4
2D	−258.0	−100.8	−265.5	−108.3	−262.7	−105.5

[a] See reference 24 for the increment values.

If this correction is applied to **1D**, **1D** becomes 9.4 kcal/mol more stable than **2L** (Table 1).

DFT (BLYP). If BLYP/6-31G*, a local nonhybrid DFT method with calculates all the correlation energy, is used to optimize geometries, the localized **1L** and **2L** structures are no longer stationary points and collapse to the delocalized **1D** and **2D** (Figure 5). **1D** is 15.6 kcal/mol more stable than **2D**. Bond length equalization is exaggerated compared to the delocalized experimental *syn* structure (**1**): the Julg parameters are A = 0.99 (**1D**) and 0.99 (**2D**), compared to the experimental value of A = 0.97 (**1**). The maximum deviation Δr_m is only 0.02 and 0.01 Å, compared to 0.03 Å obtained experimentally for

TABLE 4: GIAO-SCF/6-31G* Calculated NICS (ppm) Values for Individual Rings in [14]Annulenes with Various Optimized Geometries (the Ring Systems Are from Left to Right as Shown in Figures 4−6)[a]

	left	central	right
RHF/6-31G*			
1L (min)	−8.9	−13.7	−4.7
1D (TS)	−17.0	−22.2	−17.0
2L (min)	−5.3	−1.5	+0.3
2D (TS)	−17.4	−17.7	−17.4
BLYP/6-31G*			
1D (min)	−18.0	−21.1	−18.0
2D (min)	−17.5	−17.4	−17.6
B3LYP/6-31G*			
1D (min)	−18.0	−21.4	−18.0
2L (min)	−7.2	−2.0	+0.1
2D (TS)	−17.6	−17.6	−17.6

[a] Min stands for energy minimum, and TS for transition state.

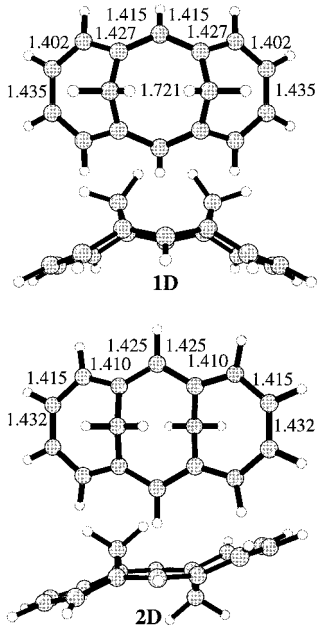

Figure 5. BLYP/6-31G* structures of the delocalized bismethano-[14]annulenes (**1D**, **2D**). Selected bond lengths are in angstroms.

the *syn* structure. The magnetic susceptibility exaltations of −96.5 and −108.3 indicate that both BLYP/6-31G* structures are aromatic. The same is true based on the calculated NICS values for **1D** (−21.1 for the central ring and −18.0 for both outer rings) and **2D** (−17.4 vs 17.5 and −17.6). The energies of the localized structures are unknown, as they cannot be located at BLYP. We can speculate that these energies are too high due to the self-interaction error, which favors delocalized structures,[5,31] and we can estimate the relative energies by BLYP/6-31G* single point calculation on the HF geometries. **1D** is predicted to be 8.5 kcal/mol lower in energy than **2L** after error correction (Table 1).

DFT(B3LYP). Both **1D** and **2L** are minima using the hybrid B3LYP/6-31G* DFT method, whereas **2D** is a transition state, in accord with experimental findings (Figure 6). However, the calculated double bond isomerization barrier for **2** (3.0 kcal/mol) is 4.1 kcal/mol lower than the experimental value (7.1 kcal/mol). The absolute error is thus the smallest found in the methods studied so far, and the difference can again be used to correct the energies of the delocalized structures. Thus, **1D** is 10.5 kcal/mol more stable than **2L** after this correction (Table 1). **1L** is not a stationary point on the B3LYP/6-31G* surface,

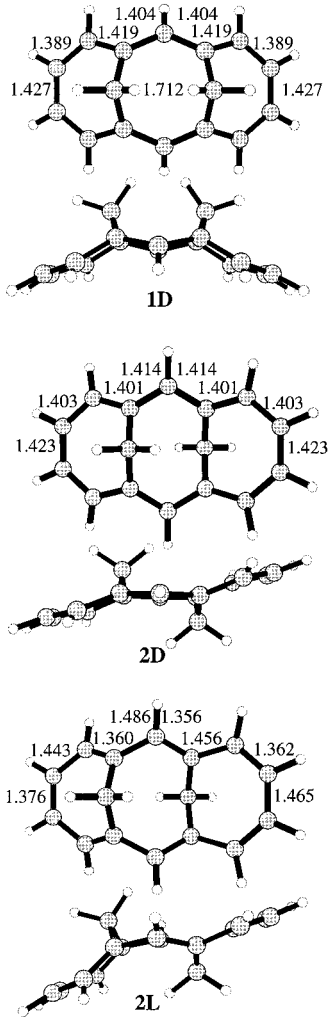

Figure 6. B3LYP/6-31G* structures of the localized (**2L**) and the delocalized (**1D**, **2D**) bismethano[14]annulenes. Selected bond lengths are in angstroms.

but a B3LYP/6-31G*//HF/6-31G* single point calculation places **1L** only 9.2 kcal/mol (5.1 kcal/mol after correction) above **1D**.

B3LYP/6-311+G**//B3LYP/6-31G* single point calculations were performed to explore basis set effects. The B3LYP/6-311+G**//HF/6-31G* energies of **1L** and **1D** have the same relative order of stability as before. The energy of **1L** is lowered to 6.2 kcal/mol relative to **1D**, **2L** is increased to 15.2 kcal/mol, and the barrier to double bond isomerization is 3.7 kcal/mol, still 3.4 kcal/mol below the experimental barrier (Table 1). After 3.4 kcal/mol error correction, **1D** is 11.8 and 2.8 kcal/mol lower in energy than **2L** and **1L**.

The Julg parameter of the localized B3LYP/6-31G* *anti* structure (**2L**, $A = 0.70$) is larger than the experimental structure (**2**, $A = 0.62$), and the delocalized *syn* structure (**1D**, $A = 0.98$) is within experimental error of the X-ray value (**1**). The magnetic susceptibility exaltations indicate that the delocalized structures are aromatic, and **2D** ($\Lambda = -105.5$) is more aromatic than **1D** ($\Lambda = -93.0$). A negligible magnetic susceptibility exaltation ($\Lambda = -6.4$) shows **2L** to be nonaromatic.[32] The NICS values for these three structures provide the same conclusions. For **1D**, the central ring NICS is −21.4 and the two outer rings have NICS = −18.0. In **2D**, all three rings have the same NICS of −17.6. On the other hand, **2L** is nonaromatic with NICS of −2.0 for the central ring and +0.1 and −7.2 for the two outer rings.

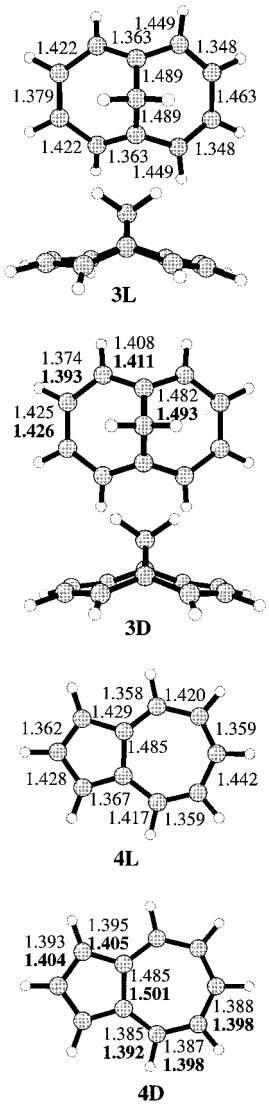

Figure 7. RHF/6-31G* structures of the localized (**3L** and **4L**) and the delocalized (**3D** and **4D**) 1,6-methano[10]annulene (**3**) and azulene (**4**). Selected RHF/6-31G* and B3LYP/6-31G* (bold) bond lengths are in angstroms.

Summary of Results for 1 and 2. As summarized in Table 1, PM3 and HF favor localized structures. Consequently, the calculated double bond isomerization barriers are too high relative to the experimental value. On the other hand, MP2 and BLYP favor delocalized structures excessively: correlated single point computations on the HF-optimized transition structures give *lower* energies than the ground states. Only B3LYP gives results close to the experimental data. After error correction, all the methods indicate that **1D** is lower in energy than **2L** by 8.5−14.0 kcal/mol. The disfavored **1L** is only slightly higher in energy than **1D**, but 2.8−5.1 kcal/mol at the B3LYP level. Note that **1L** resembles **1D** rather than **2L**, and maintains much of the delocalization and aromaticity.

1,6-Methano[10]annulene (3) and Azulene (4). The 10 π bridged annulene, 1,6-methano[10]annulene, **3**, was synthesized in 1964 by Vogel. A variety of semiempirical and ab initio calculations are available, most aimed at comparisons of bicyclic and tricyclic valence isomers, or homoaromaticity.[33] Compound **3** has been reexamined here, and the results reinforce the conclusions derived here for the [14]annulene system.

With RHF/6-31G*, the localized C_s structure (**3L**) with alternating single and double bonds is an energy minimum; and the C_{2v} delocalized structure with almost equalized bond lengths is a transition state (**3D**). Structure **3L** is only 0.2 kcal/mol more stable than **3D**. With B3LYP/6-31G*, **3D** becomes the energy minimum, and **3L** is no longer a stationary point. This holds true for the BLYP/6-31G* calculations as well. B3LYP/6-31G*//HF/6-31G* single point calculations estimate **3D** to be 4.1 kcal/mol more stable then **3L**. The Julg parameter for **3L** at HF/6-31G* is 0.79 compared to 0.95 (0.99 at BLYP/6-31G*, 0.98 at B3LYP/6-31G*, and 0.97 for the X-ray structure)[34] for **3D** and 0.95 for naphthalene[20] (the B3LYP/6-31G* Julg parameter of naphthalene is 0.95). The maximum deviations are Δr_m = 0.06 Å (**3L**) and 0.03 Å (**3D**), respectively, compared to 0.02 Å for the X-ray data and 0.03 Å for naphthalene. For the localized RHF/6-31G* structure (**3L**), the NICS values for the formal hexatriene and hexadiene units are −16.4 and −10.0. They are smaller than those for the delocalized B3LYP/6-31G* structure which are −17.7 for both formal six membered rings. Thus the localized **3L** is aromatic, albeit less than **3D**.

TABLE 5: RHF/6-31G* Relative Energies (E_{rel}, in kcal/mol), Julg Parameter (*A*, Unitless) and Maximum Deviation of the Average Bond Length (Δr_m, in angstroms) as Well as NICS Values for Methano[10]annulene (3) and Azulene (4) Compared with the Corresponding BLYP/6-31G* (in italics) and B3LYP/6-31G* (in Bold) Data

	RHF/6-31G*, (*BLYP/6-31G**), **B3LYP/6-31G***				
	E_{rel}	*A*	Δr_m	NICS(l)[b]	NICS(2)[b]
localized (**3L**)	0.0	0.79	0.06	−16.4	−10.0
delocalized (3D)	0.2	0.95	0.03		
		0.99	*0.02*		
		0.98	**0.02**	**−17.7**	**−17.7**
naphthalene[a]		0.95	0.03		
		0.95	**0.04**	**−11.4**	**−11.4**
localized (**4L**)	0.0	0.87	0.04	−18.1	−5.9
delocalized (**4D**)	0.4	1.00	0.01		
		1.00	**0.01**	**−21.5**	**−8.3**

[a] Reference 26. [b] NICS(1) is located at the geometrical center of the hexatriene subunit and NICS(2) for the hexadiene moiety in **3L**. In **3D** and naphthalene, NICS(1) and NICS(2) are equal. In azulene (**4**), NICS(1) refers to the five-membered ring and NICS(2) to the seven-membered ring.

In contrast to 1,6-methano[10]annulene (**3**), azulene (**4**) has been investigated at many computational levels.[35,36] As expected, RHF/6-31G* favors the localized (**4L**) geometry in C_s symmetry with strong bond length alternation by 0.4 kcal/mol; the C_{2v} delocalized structure (**4D**) is the transition state for the double bond isomerization. At more sophisticated levels (MP2 and MR-SDCI), **4L** becomes higher in energy than **4D**, although by less than 4 kcal/mol.[36] These results are reproduced by our B3LYP/6-311+G** computations. With B3LYP/6-311+G**, the localized **4L** disappears upon optimization and the delocalized **4D** is the true energy minimum (the lowest vibrational frequency is 163 cm^{-1}), and **4L** (single point B3LYP/6-311+G**//HF/6-31G*) is 2.6 kcal/mol higher in energy than **4D**. The computed Julg parameter of **4L** is smaller than that of the delocalized structure (**4D**) at both HF and B3LYP levels (Table 5). On the basis of the results of the localized **1L** and **3L**, which are both aromatic, the localized azulene **4L** is expected to be aromatic as well. The NICS values for the five- and seven-membered in **4L** of −18.1 and −5.9 indicate the aromatic character as compared with the values of **4D** (−21.5 vs −8.3).

Consequences

All the common quantum mechanical methods employed, PM3, RHF, BLYP, and B3LYP, have some systematic difficul-

ties in reproducing experimental geometries and energies of the aromatic systems examined here. B3LYP/6-31G* calculations perform best; the combination of Hartree−Fock with Kohn−Sham exchange balances errors of opposite sign in the relative energies of localized and delocalized structures.

Finally, we turn to the issue of the origin of bond length equalization, which we have referred to as delocalization. When a π system is planar or nearly so, cyclic delocalization can occur. Both localized and delocalized structures may be quite similar in energy, and optimization with methods including correlation energy will find a delocalized (bond-equalized) geometry. For example, **1L** is just 2.8 kcal/mol (B3LYP/6-311+G**//RHF/6-31G*) higher in energy than **1D**, but only the latter is found by MP2 or DFT, and only **1D** is known experimentally. On the basis of magnetic criteria, **1L** is aromatic, but significantly less than **1D**. This behavior is also illustrated by 1,6-methano-[10]annulene (**3**) and by azulene (**4**), where electron correlated methods provide solely delocalized minima. When the σ system allows π overlap, σ and π preferences work together to equalize bond lengths. However, the aromatic stabilization energies for such systems are not large, and strain can become the determining factor in the optimized structures. Such strain effect may reduce aromaticity or even eliminate it entirely as observed in **2**.

Due to the buckle of the σ skeleton, the π overlap in the nonaromatic *anti* structure (**2L**) is reduced to such an extent that bond length localization results. Planarization of the σ skeleton in **2L** to give transition state **2D** allows effective π overlap and permits bond length equalization. However, this species is destabilized by the angle strain of the skeleton. Thus, the interplay between σ and π systems may result in two different situations: (a) σ and π may work together and lead to delocalized structures with equalized bond lengths as in **1**−**4D**; (b) the geometrical requirement of the σ skeleton may dominate and resulting geometries may preclude effective π overlap; nonaromatic structures like **2L** result. The maximum angle between π orbitals which still permits delocalization is about 30° in the case of the RHF/6-31G* optimized structures. It is 34° in **1L**, 28° in **1D**, −79° in **2L**, and −34° in **2D**.

Conclusions

The substantial π delocalization of the *syn* bis-methano[14]-annulene (**1**) does not overcome the inherent preference for localization in the RHF and PM3 calculations. While RHF theory favors localized structures and underestimates the delocalization energy by 2.8 kcal/mol per electron pair in **2D**, hybrid density functional theory (B3LYP/6-31G*) provides correct geometries, but overestimates delocalization by −0.6 kcal/mol per electron pair for aromatic systems. B3LYP is the method of the choice for computing delocalized and polyenic systems. After error correction, the *syn* delocalized structure **1D** was computed to be the global energy minimum, 11.8 kcal/mol below the *anti* localized **1L** at the B3LYP/6-311+G** level.

In agreement with the X-ray structures and ^{1}H-NMR chemical shifts, the *syn* structure (**1D**) is highly aromatic with a large (negative) magnetic susceptibility exaltation and negative NICS values. Based on the same criteria, the *anti* minimum (**2L**) is nonaromatic.

Acknowledgment. We are grateful to the National Science Foundation for financial support of this research and to the San Diego Supercomputer Center for computational support at UCLA and to the Deutsche Forschungsgemeinschaft (DFG), as well as to the Fonds der Chemischen Industrie in Erlangen.

References and Notes

(1) (a) Minkin, V. I.; Glukhovtsev, M. N.; Simkin, B. Y. *Aromaticity and Antiaromaticity*; Wiley: New York, 1994. (b) Garatt, P. J. *Aromaticity*; Wiley: New York, 1986. (c) Schleyer, P. v. R.; Jiao, H. *Pure Appl. Chem.* **1996**, *68*, 209.

(2) Schleyer, P. v. R.; Freeman, P. K.; Jiao, H.; Goldfuss, B. *Angew. Chem., Int. Ed. Engl.* **1995**, *34*, 337.

(3) Schleyer, P. v. R.; Dransfeld, A.; Maerker, C.; Jiao, H.; Van E. Hommes, N. J. R. *J. Am. Chem. Soc.* **1996**, *118*, 6317.

(4) (a) Shurki, A.; Shaik, S. *Angew. Chem., Int. Ed. Engl.* **1997**, *36*, 2205. (b) Hiberty, P. C.; Danovich, D.; Shurki, A.; Shaik, S. *J. Am. Chem. Soc.* **1995**, *117*, 7760. (c) Kutzelnigg, W. *Einführung in die Theoretische Chemie*; Verlag Chemie: New York, 1978; Vol. 2, p 318. (d) Aihara, J. *Bull. Chem. Soc. Jpn.* **1990**, *63*, 1956. (e) Gobbi, A.; Yamaguchi, Y.; Frenking, G.; Schaefer, H. F., III. *Chem. Phys. Lett.* **1995**, *117*, 9559.

(5) Glendening, E. D.; Faust, R.; Streitwieser, A.; Vollhardt, K. P. C.; Weinhold, F. *J. Am. Chem. Soc.* **1993**, *115*, 10952.

(6) Plattner, D. A.; Houk, K. N. *J. Am. Chem. Soc.* **1995**, *117*, 4405.

(7) (a) Taylor, P. R.; Bylaska, E.; Weare, J. H.; Kawai, R. *Chem. Phys. Lett.* **1995**, *235*, 558. (b) Martin, J. M. L.; Taylor, P. R. *Chem. Phys. Lett.* **1995**, *240*, 521. (c) Nendel, M.; Houk, K. N.; Tolbert, L. M.; Vogel, E.; Jiao, H.; Schleyer, P. v. R. *Angew. Chem., Int. Ed. Engl.* **1997**, *36*, 748. (d) Choi, C. H.; Kertesz, M. *J. Chem. Phys.* **1998**, *108*, 6681; *J. Phys. Chem. A* **1998**, *102*, 3429. (e) Choi, C. H.; Kertesz, M.; Karpfen, A. *J. Am. Chem. Soc.* **1997**, *119*, 11994. (f) Goldfuss, B.; Schleyer, P. v. R. *Organometallics* **1995**, *14*, 1553. (g) Goldfuss, B.; Schleyer, P. v. R.; Hampel, I. *Organometallics* **1996**, *15*, 1755. (h) Goldfuss, B.; Schleyer, P. v. R. *Organometallics* **1997**, *16*, 1543.

(8) (a) Mitchell, R. H.; Chen, Y.; Iyer, V. S.; Lau, D. Y. K.; Baldridge, K. K.; Siegel, J. S. *J. Am. Chem. Soc.* **1996**, *118*, 2907. (b) Borden, W. T.; Davidson, E. R. *Acc. Chem. Res.* **1996**, *29*, 67.

(9) Sulzbach, H. M.; Schaefer III, H. F.; Klopper, W.; Lüthi, H. P. *J. Am. Chem. Soc.* **1996**, *118*, 3519.

(10) Disch, R. L.; Schulman, J. M. *Chem. Phys. Lett.* **1988**, *152*, 402.

(11) Pedley, J. B.; Naylor, R. D.; Kirby, S. P. *Thermochemical Data of Organic Compounds*, 2nd ed.; Chapman and Hall: London, 1986.

(12) Jiao, H.; Schleyer, P. v. R. *Angew. Chem.* **1996**, *108*, 2548; *Angew. Chem., Int. Ed. Engl.* **1996**, *35*, 2383.

(13) Vogel, E.; Sombroek, J.; Wagemann, W. *Angew. Chem., Int. Ed Engl.* **1975**, *14*, 564.

(14) Vogel, E.; Haberland, U.; Günther, H. *Angew. Chem., Int. Ed Engl.* **1970**, *9*, 513.

(15) Destro, R.; Pilati, T.; Simonetta, M. *Acta Crystallogr. B* **1977**, *B33*, 940.

(16) Gramacioli, C. M.; Mimun, A. S.; Mugnoli, A.; Simonetta, M. *J. Am. Chem. Soc.* **1973**, *95*, 3149.

(17) Frisch, M. J.; Trucks, G. W.; Schlegel, H. B.; Gill, P. M. W.; Johnson, B. G.; Robb, M. A.; Cheeseman, J. R.; Keith, T. A.; Peterson, G. A.; Montgomery, J. A.; Raghavachari, K.; Al-Laham, M. A.; Zakrzewski, V. G.; Ortiz, J. V.; Foresman, J. B.; Cioslowski, J.; Stefanov, B. B.; Nanayakkara, A.; Challacombe, M.; Peng, C. Y.; Ayala, P. Y.; Chen, W.; Wong, M. W.; Andres, J. L.; Replogle, E. S.; Gomperts, R.; Martin, R. L.; Fox, D. J.; Binkley, J. S.; Defrees, D. J.; Baker, J.; Stewart, J. P.; Head-Gordon, M.; Gonzalez, C.; Pople, J. A. *Gaussian 94*; Gaussian, Inc.: Pittsburgh, PA, 1995.

(18) For Macromodel V5.0, see: Mohamadi, F.; Richards, N. G. J.; Guida, W. C.; Liskamp, R.; Camfield, C.; Chang, G.; Hendrickson, T.; Still, W. C. *J. Comput. Chem.* **1990**, *11*, 440.

(19) Pople, J. A.; Scott, A. P.; Wong, M. W.; Radom, L. *Isr. J. Chem.* **1993**, *33*, 345.

(20) Julg, A.; François, P. *Theor. Chim. Acta* **1967**, *8*, 249.

(21) Dauben, H. J., Jr.; Wilson, J. D.; Laity, J. L. in *Non-Benzenoid Aromatics*; Synder, J., Ed.; Academic Press: New York, 1971; Vol. 2 and references cited therein. For further applications, see: (a) Jiao, H.; Schleyer, P. v. R.; Glukhovtsev, M. N. *J. Phys. Chem.* **1996**, *100*, 12299. (b) Jiao, H.; van E. Hommes, N. J. R.; Schleyer, P. v. R.; de Meijere, A. *J. Org. Chem.* **1996**, *61*, 2826. (c) Jiao, H.; Schleyer, P. v. R.; Mo, Y.; McAllister, M. A.; Tidwell, T. T. *J. Am. Chem. Soc.* **1997**, *119*, 7075.

(22) Jiao, H.; Schleyer, P. v. R. *AIP Conference Proceedings 330*, E.C.C.C.1, *Computational Chemistry*, Bernardi, F., Rivail, J.-L., Eds.; American Institute of Physics: Woodbury, New York, 1995; p 107.

(23) (a) Kutzeluigg, W. *Isr. J. Chem.* **1980**, *19*, 193. (b) Schindler, M.; Kutzelnigg, W. *J. Chem. Phys.* **1982**, *76*, 1910. (c) Kutzelnigg, W.; Fleisher, U.; Schindler, M. *NMR, Basic Principles and Progress*; Springer Verlag: Berlin, 1990; Vol. 23, p 165.

(24) Jiao, H.; Nagelkerke, R.; Kurtz, H. A.; Williams, R. V.; Borden, W. T.; Schleyer, P. v. R. *J. Am. Chem. Soc.* **1997**, *119*, 5921. The IGLO/DZ increment values (in ppm cgs) are −17.8 (Me), −14.8 (>CH_2), −11.5 (>CH−), −7.6 (>C<), −10.0 (−CH=) and −6.9 (>C=).

(25) Brock, C. P.; Dunitz, J. D. *Acta Crystallogr.* **1990**, *B46*, 795.

(26) Brock, C. P.; Dunitz, J. D. *Acta Crystallogr.* **1982**, *B38*, 2218.

(27) Bühl, M.; Thiel, W.; Jiao, H.; Schleyer, P. v. R.; Saunders, M.; Anet, F. A. L. *J. Am. Chem. Soc.* **1994**, *116*, 6005.

(28) There are 30 bond lengths of 1.38 Å and 60 of 1.45 Å. Diederich, F.; Thilgen, F. *Science* **1996**, *271*, 317.

(29) Houk; K. N.; Li, Y.; Evanseck, J. D. *Angew. Chem., Int. Ed Engl.* **1992**, *31*, 682.

(30) MP2/6-31G* single point computations also have been performed on the HF/6-31G* geometries, even though the delocalized anti (**2D**) RHF/6-31G* wavefunction was found to be unstable with respect to the UHF wavefunction. MPn energies are not reliable if the wave functions are unstable (Cársky, P.; Hubač, I. *Theor. Chim. Acta* **1991**, *80*, 407), but such calculations are nevertheless often performed. Since the optimized UHF wave functions were highly spin-contaminated, UMP2 calculations were not pursued.

(31) Johnson, B. G.; Gonzales, C. A.; Gill, P. M. W.; Pople, J. A. *Chem. Phys. Lett.* **1994**, *221*, 100.

(32) This small exaltation (−6.4) and the NICS (−7.2) for the outer ring are ascribed to the slightly homoaromatic character of the cycloheptatriene moiety of the *anti* localized structure (**2L**). For a discussion of cycloheptatrienes: Jiao, H.; Schleyer, P. v. R. Manuscript in preparation.

(33) (a) Farnell, L.; Radom, L. *J. Am. Chem. Soc.* **1982**,*104*, 7650. (b) Cremer, D.; Dirk, B. *Angew. Chem., Int. Ed. Engl.* **1982**, *21*, 869. (c) Haddon, R. C.; Raghavachari, K. *J. Am. Chem. Soc.* **1985**, *107*, 289. (d) Catti, C.; Barzaghi, M.; Simonetta, M. *J. Am. Chem. Soc.* **1985**, *107*, 878. (e) Simonetta, M.; Barzaghi, M.; Gatti, C. *J. Mol. Struct. (THEOCHEM)* **1986**, *138*, 39. (f) Bock, C. W.; George, P.; Gluster, J. P. *J. Mol. Struct. (THEOCHEM)* **1991**, *234*, 227. (g) George, P.; Clusker, J. P.; Bock, C. W. *J. Mol. Struct. (THEOCHEM)* **1991**, *235*, 193. (h) Sironi, M.; Raimondi, M.; Copper, D. L.; Gerratt, J. *J. Mol. Struct. (THEOCHEM)* **1995**, *338*, 257. (i) Mealli, C.; Ienco, A.; Boyt, E. B. Jr.; Zoellner, R. W. *Chem. Eur. J.* **1997**, *3*, 958.

(34) Bianchi, R.; Pilati, T.; Simonetta, M. *Acta Crystallogr.* **1980**, *B36*, 3146.

(35) Negri, F.; Zgierski, M. Z. *J. Chem. Phys.* **1993**, *99*, 4318. (b) Peck, R. C.; Schulman, J. M.; Disch, R. L. *J. Phys. Chem.* **1990**, *94*, 6637. (c) Morley, J. O. *J. Chem. Soc., Perkin Trans. 2* **1989**, 103. (d) Haddon, R. C.; Raghavachari, K. *J. Chem. Phys.* **1983**, *79*, 1093. (e) Haddon, R. C.; Raghavachari, K, *J. Am. Chem. Soc.* **1982**, *104*, 3516.

(36) Grimme, S. *Chem. Phys. Lett.* **1993**, *201*, 67.